

TIME-FREQUENCY ANALYSIS OF TRANSIENT VIBRATIONS TO IMPROVE TURBO-COMPRESSOR START-UP

Juan C. Jauregui
CIATEQ, A.C.
Unidad Aguascalientes
Aguascalientes, México
Phone: +52(449)9731060
e-mail: [jcyjaur@ciateq.mx](mailto:jcjaur@ciateq.mx)

Oscar Gonzalez
CIATEQ, A.C.
Unidad Aguascalientes
Aguascalientes, México
Phone: +52(449)9731060
e-mail: oscarm@ciateq.mx

Eduardo Rubio
CIATEQ, A.C.
Unidad Aguascalientes
Aguascalientes, México
Phone: +52(449)9731060
e-mail: eduardo.rubio@ciateq.mx

ABSTRACT

Diagnosis of turbo-compressors during start-up is a particularly challenging task. One of the reason is the reduced set of instruments that monitor this procedure. It is cumbersome to adjust lubrication and steam valves while controlling the speed and dynamic stability. In order to get the turbo-compressor out of a high vibration zone, it is important to be able to predict instabilities associated to the start-up process. Thus, it is necessary to have a measurement system with the ability of fault detection, especially at early stages of fault appearance. In this way, the start-up time can be significantly reduced. Although recent developed diagnosis methods use information from different sources and measurements, data structures are not designed to carry predictive information related to the turbo-compressor health. Therefore, it is important to extract early warning signals related to instability conditions. Vibration signals during machine start-up are non-stationary in nature, and conventional techniques, such as Fourier transforms and time series analysis, have difficulties to extract the full features of the vibrations signature. In this paper, the features of start-up vibrations in rotational systems like those found in turbo compressors are investigated by time-frequency analysis, and appropriate analysis of the transient vibration during compressor start-up is presented.

INTRODUCTION

The start-up of a turbo-compressor is a series of procedures that must be carefully performed in order to get the system into normal operations. This process, which might take several days, involves many activities that require practical experience, judgment and engineering guidance. For example, the reference document for the writing of this procedure is

ASME PTC-10 [1]. Among the checking points of a typical start-up procedure, the more important ones are:

1. Verify that the instrumentation is properly calibrated
2. Circulate the oil through the lubrication and seal lines. Bypass or remove seals.
3. Replace oil filters, clean reservoirs and fill with proper oil.
4. Reinstall bearings and seals.
5. Bring the lubrication system to proper pressure and temperature levels.
6. Verify protection equipment both at operating point and at emergency (seal protection, high temperature, low voltage, vibration sensors, lubrication pumps, etc.)
7. Blow down the steam line
8. Verify turbine inlet and temperature gauges.
9. Run the turbine uncouple from the compressor.
10. If possible, run the compressor with air prior to process gas.

The procedure for bringing the steam turbine into speed is conducted according to manufacturer specifications. Typically, it starts by warming up the turbine without load, at a speed of 500 rpm, once it reaches operating temperatures, the speed is gradually increased. Passage through its critical speed must be done fast.

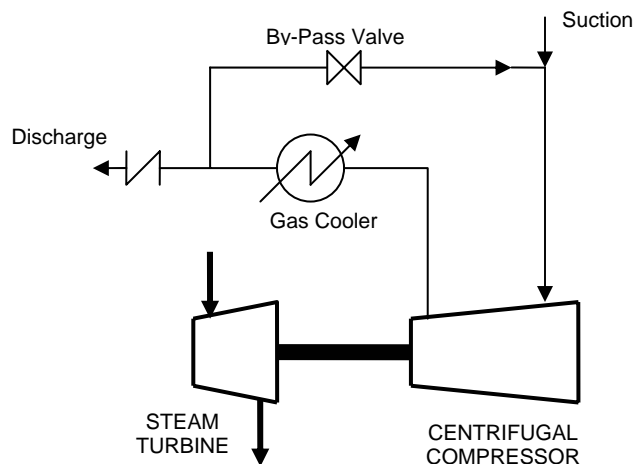


Figure 1. Steam turbine driven centrifugal compressor system.

taken on the dynamic behavior. Since it depends on load and speed, careless speed increments may result in high vibrations; therefore, the start-up time is incremented until the vibrations get to an acceptable level.

The typical components of a steam turbine system are shown in Fig. 1, while Fig. 2 sketches how the steam turbine and the compressor are integrated.

Although machinery monitoring systems have been applied for many years [2], they are unable to identify transient problems during compressor start-up. The reason is that they are based on FFT (Fast Fourier Transform), and, due to its principle, this function can not analyze non-linear neither transient vibrations. Recently, time-frequency functions have been studied as an alternate way to analyze such vibration problems. Smalley [4] indicates that if the time span of the transient vibration is known, the compressor speed should be increased at shorter intervals since the acceleration rate is a factor which controls the magnitude of vibrations. It is also in this stage that non-linear and transient problems are often found during attempts to bring a compressor up to speed. That is why an appropriate analysis of the transient vibration during compressor start-up is needed.

The application of wavelet transform to vibration and diagnosis has been widely studied. Newland [5] proposed the application of harmonic wavelets to the creation of time- The ability to gradually increase speed provides the operator with time to verify and adjust any parameter before any speed increment.

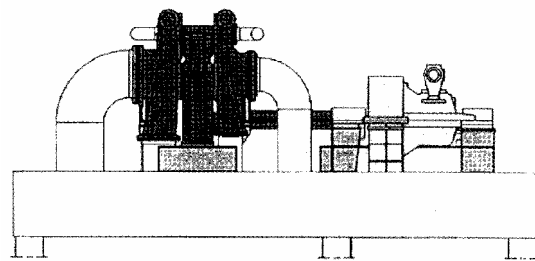


Figure 2. Steam turbine driven centrifugal compress

Once the thermal conditions are stabilized, care must be frequency maps. In this way, it is possible to trace the spectral content of a signal as it changes with time. A similar work presented by Zheng and McFadden [6] demonstrated that bilinear time-frequency distributions could provide high resolutions in time domain and frequency domain at the same instant. They originally proposed a combination of Cohen's and Wigner's distributions. Staszewski [7] analyzed various types of wavelets and presented procedures for an adequate selection of wavelet coefficients for the analysis of vibration signals.

White [8] analyzed deterministic and stochastic non-stationary signals with different time-frequency distributions, Wigner-Ville distributions and Cohen distribution. Kim [9] proposed the application of Analytic Wavelet Transform (AWT) for the identification of temporal variations of the spectral energy. The application of AWT is an ideal time-frequency tool because it combines both Fourier and wavelet transform. Using this function, they studied its application to risk assessment methods. Sanz [10] presented another approach by combining the wavelet transform with an auto-associative neural network. The generated data sets in an unsupervised mode, train the neural networks with wavelet coefficients of healthy signals, and afterwards, they used these networks for the identification of faulty signals. Cole [11, 12] applied wavelet transform as a basis for the control of rotor vibration. Vibration signal wavelet coefficients that relate to different time scales provide direct information on the system dynamic state, and can thus be used for feedback in a closed-loop control strategy that attenuates both transient and steady-state vibration components. Control force signals are synthesized from basis functions having a characteristic frequency and spacing interval closely matched to the rotational frequency.

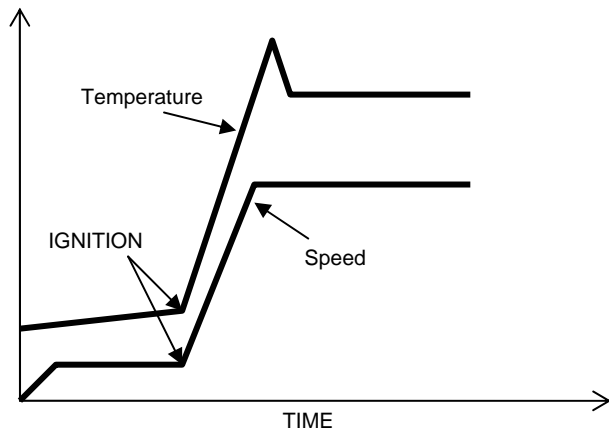


Figure 3. Start-up characteristics of a gas turbine.

Jiang [13] studied conditioning monitoring and fault diagnosis with a time-frequency map built with a wavelet transform. They applied the Morlet wavelet and were able to identify singularities, faults, and trends; they also could perform prognosis. A similar study was presented by Liu [14], where he showed a method that overcomes the limitations of Coifman and Wickerhauser's algorithm. In this way he detected hidden transients in early stages of fault development. Kawada [15] and Wan [16] showed the application of wavelet transform to the vibration diagnosis of turbine generators. They showed its advantages for the identification of unsteady and non-linear effects.

Other papers deal with different applications of wavelet transform, such as loose blade identification [16], and transient patterns [17, 18].

NOMENCLATURE

A	stage gain
A/D	analog to digital converter
G	details branch
H	smoothing branch
LPF	low pass filter
N	normal
OL	open loop
Q	quantization stage
T	time step, tangential
W	wavelet transform
Z	domain transformation
f()	function
i	input

j	complex
n	index
o	output
s	scale parameter, sampling, stator
t	time
u	translation parameter
x	signal, rotor displacement
*	Complex conjugate
β	feedback gain
ρ	unbalance radius
ϕ	angle
ψ	wavelet function
$\hat{\psi}$	Fourier Integral Transform of ψ
ω	angular frequency

FIELD PROBLEM

The procedure presented in this work came from a field case. A natural gas compressor of a Cryogenic plant was rebuilt. Its rotor, seals and bearings were renewed. This compressor is driven by a steam turbine, as shown in Fig. 1.

Once the machine was commissioned for operation, the rotor presented high axial vibration. Its stabilization consumed an enormous amount of time. The main problem was due to the fact that the instrumentation was only able to analyze the RMS value, so no tendency was able to be predicted. As a consequence, a detailed analysis of actual data was simply impossible.

Figure 4 shows the axial vibration data. It is possible to see that after one hour, the axial vibration surpassed the value of 10.1 mm/s (0.4 in/s), and it took almost five hours to stabilize the system. In order to validate the rebuilt, the compressor was stopped and the alignment of the compressor and turbine checked again. The flexible couple, all seals and bearings were also inspected to verify if there were any damage.

A second start-up was carried out. This time, however, the start-up axial vibration never surpassed the 7.6 mm/s (0.3 in/s) threshold and the compressor was stabilized just after two hours, as shown in Fig. 5.

This field problem demonstrated that with good knowledge of the transient response, the first start-up would have been easier, faster and without exposing the compressor to unnecessary high vibrations.

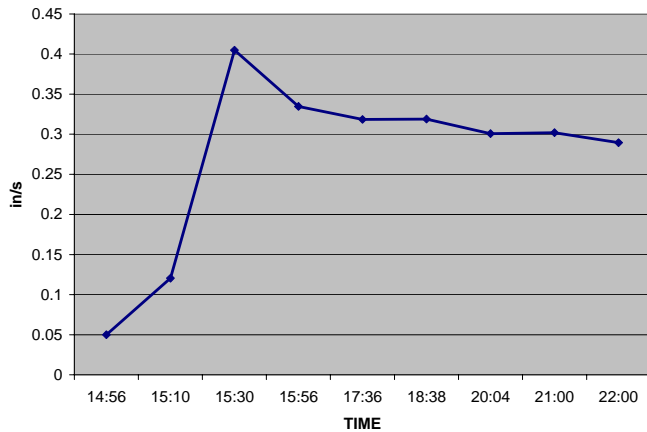


Figure 4. Axial vibration during first start-up

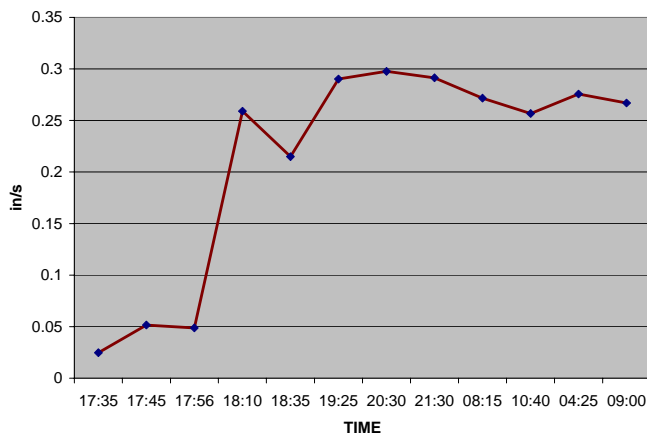


Figure 5. Axial vibration during second start-up

Table 1. Experimental procedure parameters

No	Pressure	Load	Time span
1	6.9 kPa	Low	10 sec
2	10.3 kPa	Low	10 sec
3	13.8 kPa	Low	10 sec
4	6.9 kPa	Medium	10 sec
5	10.3 kPa	Medium	10 sec
6	13.8 kPa	Medium	10 sec
7	6.9 kPa	Full	10 sec
8	10.3 kPa	Full	10 sec
9	13.8 kPa	Full	10 sec
10	6.9 kPa	Low	2 sec
11	10.3 kPa	Low	2 sec
12	13.8 kPa	Low	2 sec
13	6.9 kPa	Medium	2 sec
14	10.3 kPa	Medium	2 sec
15	13.8 kPa	Medium	2 sec
16	6.9 kPa	Full	2 sec
17	10.3 kPa	Full	2 sec
18	13.8 kPa	Full	2 sec

The lubricant pressure on the journal bearing was run at 6.9 kPa, 10.3 kPa and 13.8 kPa. For each bearing pressure run, the system was loaded at: low, medium and full shaft load. The last parameter was the stabilization time. It was set for 10 seconds and 2 seconds for each set arrangement. Thus, the test resulted in a total combination of 18 runs, as Table 1 indicates.

The acceleration ramp was performed from a velocity of 500 rpm to a maximum velocity of 7,000 rpm with increments of 500 rpm every 10 seconds and 2 seconds depending on the case. Once the maximum velocity was reached, the system was then slowed down, again in decrements of 500 rpm in order to verify if any hysteresis was happening in the critical speeds values when speeding up or slowing down.

EXPERIMENTAL PROCEDURE

In order to develop an analysis tool for the transient response during compressor start-up, an experimental procedure was carried on. This experiment was performed using a rotor-kit, in which the variables were: lubricant pressure on the journal bearing, load on the system and the time to stabilize the system during an acceleration ramp, thus simulating the compressor start-up.

The rotor-kit has the advantage of being a compact model of a rotating machine, able to simulate several categories of lateral shaft vibration by duplicating vibration-producing phenomena found in large rotating machine.

The vibration measurement was performed using a ADXL-311, 2-axis accelerometer, mounted on the bearing next to the motor, and filtered by data acquisition board

SIGNAL ANALYSIS

Low level signals from the sensor pickup were amplified before being converted to digital form. This process is shown in Fig. 6 where the block A_{OL} represents an amplifier's open loop gain. The input to the amplifier, x_i , was the difference between the input source signal and the output of the feedback. The output of this stage is:

$$x_0 = A_{OL}(j\omega) \cdot (x_a - x_f) \quad (1)$$

The output signal is altered by a feedback factor:

$$x_f = \beta \cdot x_0 \quad (2)$$

The amplified signal is then passed to a digital conversion process where an anti-aliasing filter (LP) with a cutoff

frequency ω , ensures a bandwidth limited signal and determines feasible sampling intervals T_s . A quantization stage is used to obtain the digital signal:

$$x(n) = Q[x(nT_s)] \quad (3)$$

In mathematical terms, a wavelet is a function with zero average:

$$\int_{-\infty}^{+\infty} \psi(t) dt = 0 \quad (4)$$

which is dilated by a scale parameter s , and translated by u :

$$\psi_{u,s}(t) = \frac{1}{\sqrt{s}} \psi\left(\frac{t-u}{s}\right) \quad (5)$$

Wavelet transform of a function f at the scale s and position u is computed by correlating f with a wavelet atom:

$$Wf(u,s) = \int_{-\infty}^{+\infty} f(t) \frac{1}{\sqrt{s}} \psi^*\left(\frac{t-u}{s}\right) dt \quad (6)$$

Wavelet transforms can measure time-frequency variations of spectral components, but with a different time-frequency resolution. A wavelet transform correlates f with $\psi_{u,s}$, and it can also be written as a frequency integration:

$$Wf(u,s) = \int_{-\infty}^{+\infty} f(t) \psi_{u,s}^*(t) dt = \frac{1}{2\pi} \int_{-\infty}^{+\infty} f(\omega) \hat{\psi}_{u,s}^*(\omega) d\omega \quad (7)$$

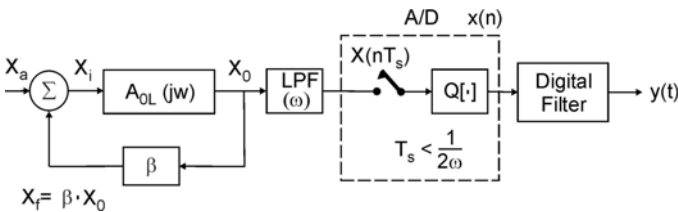


Figure 6. Digital signal processing

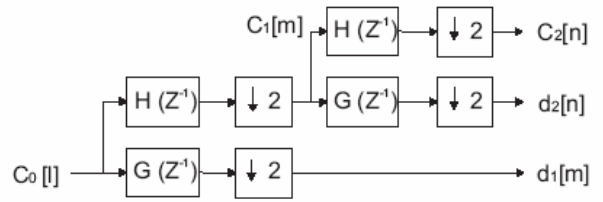


Figure 7. Wavelet processing algorithm

The wavelet coefficient $Wf(u,s)$ depends on the values $f(t)$ and $\hat{f}(\omega)$ in the time-frequency region where the energies of $\psi_{u,s}$ and $\hat{\psi}_{u,s}$ are concentrated. Time varying harmonics are detected from the position and scale of high amplitude wavelet coefficients. The wavelet transform detects transients with a zooming procedure. A wavelet coefficient $Wf(u,s)$ measures the variation of f in a neighborhood of u whose size is proportional to s . Sharp signal transitions create large amplitude wavelet coefficients; singularities are detected by following the local maxima of the wavelet transform across scales.

Signal analysis is made with the discrete wavelet transform. This is implemented using a filter bank structure as shown in Fig. 7. This method proceeds as a pyramid algorithm where a coefficient matrix is applied hierarchically. The input sequence is decomposed into two subsequences by passing it through a low pass filter and a high pass filter and down-sampling the output of both filters by 2. The low and high pass filters are half-band filters called Conjugate Quadratic Filters. Filtering increases frequency resolution by 2 and sub-sampling reduces time resolution by 2 as well. The process is iterated on the low pass branch to obtain finer frequency resolution at lower frequencies. This sequence extracts information from the original signal by decomposing it into a series of approximations distributed over different frequency bands. The pyramid scheme is applied to the approximations or smoothed data until two coefficients are obtained. Time domain and frequency domain characteristics are preserved and the target application defines the number of decomposition sequences needed.

RESULTS

Experimental data were analyzed according to previous algorithm. Figures are presented as contour plots, where the axes are frequency and time and contour lines represent

vertical acceleration field. Only the most significant results are included for clarity of this paper.

It is interesting to note that for all cases with 10 seconds span between speed increments, there was enough time to stabilize the system for each run, with the exception when values approached the critical speed. However, for the 2 seconds span, the speed was increased before the system could pass its transient state, but since the critical speed was passed through rapidly, the amplitude of the system was kept at a low value.

This shows that a 10 seconds span procedure would guarantee the system's stability (with the exception of the critical speed area); nevertheless it would result in a less than optimum practice. On the other hand, the 2 second span procedure is far faster, but it could result in high pressure values on the journal due to the inertia of the components.

Fig. 8 shows the case when the load was low, bearing pressure was 10.35 kPa and the stabilization time between speed increments was 10 sec. It is notorious the presence of high peaks around 200 Hz. When bearing pressure was reduced, the high peaks reduced significantly (Fig. 9)

Figs. 10 and 11 show the results of the case with medium load and high pressure, for 2 sec and 10 sec stabilization steps respectively. In the first case, it can be noticed that higher peaks are around 100 Hz with high gradients in both time and frequency directions. Meanwhile, in the second case the peaks move to 150 Hz and it present a smooth gradient.

Figs. 12 and 13 show similar results for low load cases. It can be seen that at 2 sec stabilization time high peaks appear at 100Hz and the gradient is steeper than in the 10 sec case.

In this plots, it is easier to see the instants when transient signals show up, and how they vanished as time pass by. Thus, in a field problem, with adequate instruments, the stabilization time step can be easily determined

CONCLUSIONS

In order to reduce the start-up time, it is necessary to do a time-frequency map. In this map, the unstable conditions of a compressor, or any other rotor equipment, can be identified. Thus, the dynamic stabilization time can be directly measured and the speed steps can be reduced to a minimum.

Unstable conditions are time dependent, and they can not be identified with conventional monitoring systems. It is necessary to apply better signal processing methods such as wavelet transform. FFT analysis hide the transient content of the vibration signal; therefore, its dependency of the frequency reduces its capability of finding the stability time span.

In order to do a better start-up process it is recommended to use additional instrumentation, with a specific analysis system capable of performing wavelet analysis on real time. Also it is recommended to include in the acquisition system process temperature and pressure signals and bearing temperatures. In this way, correlation analysis can complement the stabilization span time.

REFERENCES

- [1] Boyce, M., 2003, Centrifugal Compressors, Penn Well, Tulsa, USA
- [2] Hayashida, R., Motter, J., McDole, K., 1991, "Turbomachinery monitoring systems capture and analyze vibration data", IEEE Computer Applications in Power 4(3), pp 38-43
- [3] Smalley, A.J., 1989, "Dynamic response of rotors to rubs during startup", Journal of Vibration, Acoustics, Stress, and Reliability in Design, ASME 111(3), pp 226-233
- [4] Newland, D.E., 1999, "Harmonic wavelets in vibrations and acoustics", Philosophical Transactions: Mathematical, Physical and Engineering Sciences (Series A) 357(1760), pp 2607-2625
- [5] Zheng, G.T., McFadden, P.D., 1999, "A time-frequency distribution for analysis of signals with transient components and its application to vibration analysis", Journal of Vibration and Acoustics, Transactions of the ASME 121(3), pp 328-333
- [6] Staszewski, W.J., 1998, "Wavelet based compression and feature selection for vibration analysis", Journal of Sound and Vibration 211(5), pp 735-760
- [7] White P.R., Tan M.H., Hammond J.K., 2006, "Analysis of the maximum likelihood, total least squares and principle component approaches for frequency response function estimation", Journal of Sound and Vibration, 290(3-5) pp 676-689
- [8] Kim, J, Welcome, D., Dong, R., Joon Song, W. , Hayden, C., 2007, "Time-frequency characterization of hand-transmitted, impulsive vibrations using analytic wavelet transform", Journal of Sound and Vibration, 308(1-2), pp 98-111
- [9] Sanz, J., Perera, R., Huerta, C , 2007, "Fault diagnosis of rotating machinery based on auto-associative neural networks and wavelet transforms, Journal of Sound and Vibration, 302 (4-5), pp 981-999
- [10] Cole, M.O.T., Keogh, P.S., Burrows, C.R., Sahinkaya, M.N., 2006, "Wavelet domain control of rotor vibration", Proceedings of the Institution of Mechanical Engineers, Part

C: Journal of Mechanical Engineering Science, 220(2), pp 167-184

- [11] Cole, M.O.T., Keogh, P.S., Burrows, C.R., Sahinkaya, M.N., 2006, "Adaptive control of rotor vibration using compact wavelets", Journal of Vibration and Acoustics, Transactions of the ASME, 128(5), pp 653-665
- [12] Jiang, D.-X., Diao, J.-H., Zhao, G., Qian, L.-J., 2005, "Study on methods of vibration fault diagnosis based on time-frequency contour map for turbine generator unit" Proceedings of the Chinese Society of Electrical Engineering 25(6), pp 146-151
- [13] Liu, B., 2005, "Selection of wavelet packet basis for rotating machinery fault diagnosis", Journal of Sound and Vibration, 284(3-5), pp 567-582
- [14] Kawada, M., Yamada, K., Yamashita, K., Isaka, K., 2004, "Fundamental study on vibration diagnosis for turbine generators using wavelet transform", 2004 IEEE PES Power Systems Conference and Exposition 3, pp 1215-1220
- [15] Wan, F., Xu, Q., Li, S., 2004, "Vibration analysis of cracked rotor sliding bearing system with rotor-stator rubbing by harmonic wavelet transform", Journal of Sound and Vibration, 271(3-4), pp 507-518
- [16] Lim, M.H., Salman Leong, M., 2003, "Diagnosis for loose blades in gas turbines using wavelet analysis", ASME, IGTI, Turbo Expo (Publication) IGTI, pp 289-297
- [17] Chancey, V.C. Flowers, G.T. Howard, C.L., 2003, "A harmonic wavelets approach for extracting transient patterns from measured rotor vibration data", Journal of Engineering for Gas Turbines and Power, 125(1), pp 81-89
- [18] Gaberson, H.A., 2002, "The use of wavelets for analyzing transient machinery vibration", Journal of Sound and Vibration, 36 (9), pp 12-17

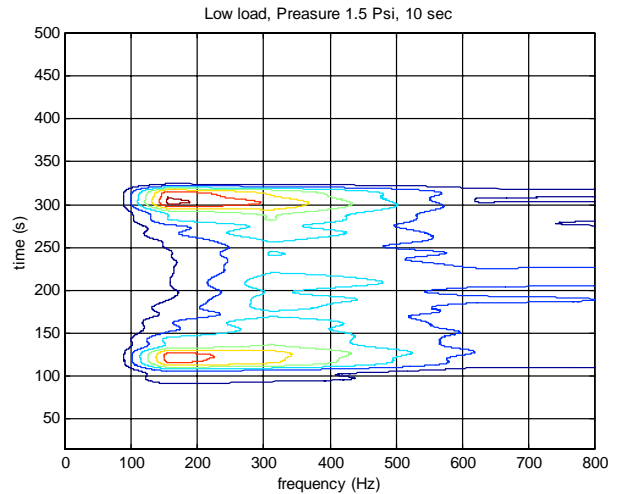


Figure 8. Time-frequency map case 1

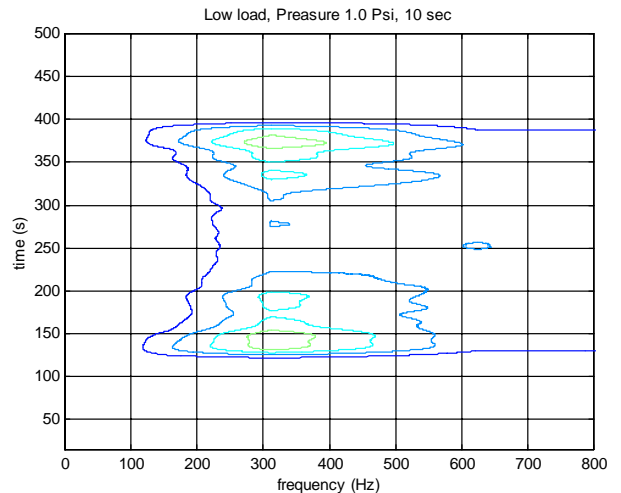


Figure 9. Time-frequency map case 2

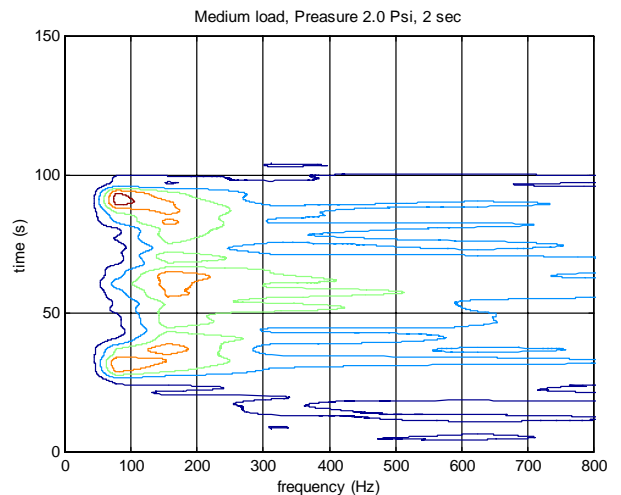


Figure 10. Time-frequency map case 3

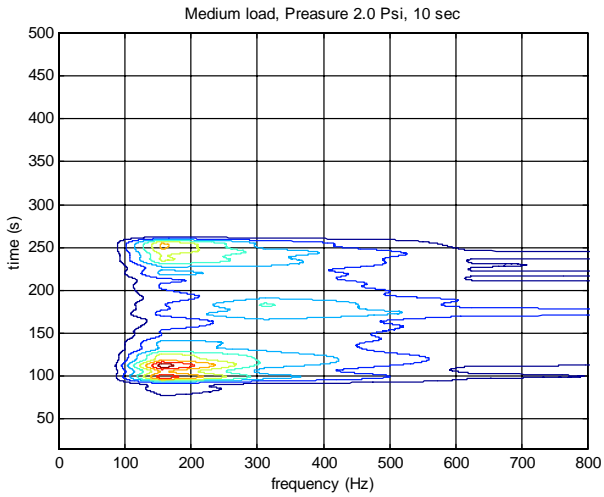


Figure 11. Time-frequency map case 4

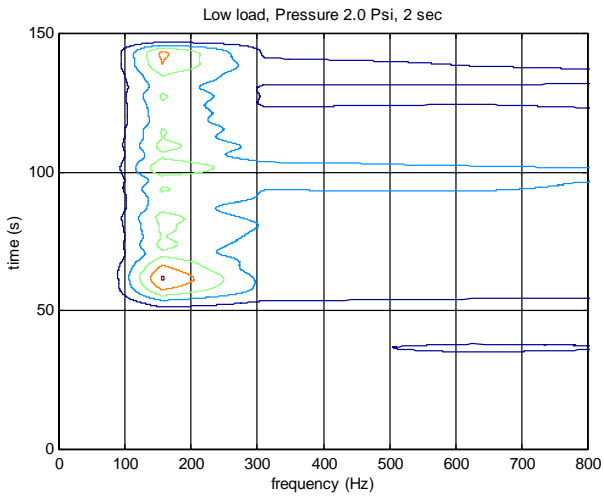


Figure 12. Time-frequency map case 5

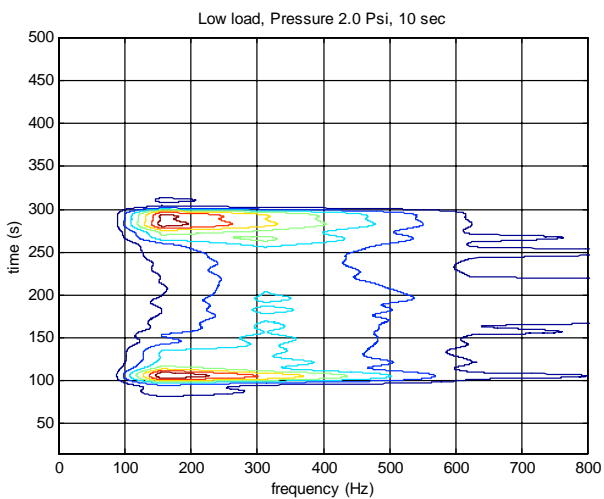


Figure 13. Time-frequency map case 6